Green Chemistry

PAPER

View Article Online
View Journal | View Issue

Open Access Article. Published on 07 February 2025. Downloaded on 10/26/2025 6:04:00 AM.
This article is licensed under a Creative Commons Attribution 3.0 Unported Licence.

Check for updates

Cite this: *Green Chem.*, 2025, **27**, 2522

Evaluating the possibilities and limitations of the pyrometallurgical recycling of waste Li-ion batteries using simulation and life cycle assessment†

Marja Rinne, Heikki Lappalainen and Mari Lundström *

Pyrometallurgical recycling of Li-ion batteries has been deemed energy-intensive and thought to result in poor recoveries, and it is typically considered disadvantageous in environmental terms in comparison to hydrometallurgical and direct recycling in the state-of-the-art literature. The process pathways for Li-ion batteries are constantly evolving, however, and such assumptions warrant re-evaluation when new technologies emerge, such as for the recovery of lithium by volatilization. The potential benefits and limitations of pyrometallurgical Li-ion battery recycling were evaluated with process simulation and life cycle assessment with and without pre-treatment stage for dismantled end-of-life batteries to demonstrate how the current processes should be developed to reach the EU's battery regulation goals. The analysis showed that the recovery of lithium by novel volatilization method followed by leaching-carbonation is environmentally viable, and that the pyrometallurgical recycling of nickel and cobalt-bearing NMC111 and NMC811 batteries results in significant impact reductions *vs.* primary raw materials especially when pre-treatment is conducted. The processing of NMC cells or black mass does not necessarily require external reducing agents or fuels due to the presence of graphite on the anode. The recycling of lithium iron phosphate (LFP) batteries, however, is more challenging. The results show that the pyrometallurgical processing of NMC batteries can satisfy both EU Battery Regulation targets assuming that the slagging of cobalt and nickel can be optimized.

Received 28th October 2024,
Accepted 3rd February 2025

DOI: 10.1039/d4gc05409a

rsc.li/greenchem

Green foundation box

1. A life cycle assessment (LCA) study of emerging pyrometallurgical methods for the recycling of lithium-ion batteries was conducted using process simulation for data generation and in the interpretation of data.
2. The recovery of lithium by volatilization appears both environmentally and technically sound, but reaching each of the recovery goals for both mass and individual elements mandated by EU Battery regulation is extremely challenging. The recycling of NMC batteries should, however, be environmentally preferable to primary metals in the majority of the assessed impact categories.
3. Further research should consider alternative pyrometallurgical processes utilizing non-carbonaceous reductants or comparison with direct hydrometallurgical processing.

1. Introduction

The rise of battery-powered electric vehicles (EVs) has led to a sharp increase in the use of lithium-ion (Li-ion) batteries, which is the currently dominant energy storage technology. This comes with several challenges: for instance, Li-ion batteries require many scarce and critical materials, including but not limited to lithium and cobalt, which are at risk for supply bottleneck already in the short and medium term.[1,2] Careful

Aalto University, School of Chemical Engineering, Department of Chemical and Metallurgical Engineering, Vuorimiehentie 2, P.O. Box 16200, FI-00076 Aalto, Finland. E-mail: mari.lundstrom@aalto.fi

† Electronic supplementary information (ESI) available. See DOI: https://doi.org/10.1039/d4gc05409a

This journal is © The Royal Society of Chemistry 2025

Open Access Article. Published on 07 February 2025. Downloaded on 10/26/2025 6:04:00 AM.
This article is licensed under a Creative Commons Attribution 3.0 Unported Licence.

end-of-life treatment of Li-ion batteries is necessary also because spent batteries are hazardous waste, but their recycling is notoriously challenging primarily due to the fire hazards and the chemical and physical heterogeneity of waste batteries.[3,4]

The current methods for the recycling of Li-ion batteries are typically divided into pyrometallurgical and hydrometallurgical approaches in literature. The division is not without flaws: the actual flowsheets consist of any combination of mechanical, pyrometallurgical, and hydrometallurgical processes, and pyrometallurgical recycling flowsheets include a substantial number of hydrometallurgical units. The processing typically starts by disassembly and pre-treatment, where the battery is usually discharged, the pack components are stripped, and the modules or cells may be crushed and mechanically treated to give an active material concentrate also known as black mass. Pre-treatment alone is complex, and each flowsheet is unique.[3,5,6]

Direct hydrometallurgical processing requires pre-treatment of the batteries to prepare black mass, which is leached and refined in aqueous media. These hydrometallurgical processes are highly tailored for a specific raw material. Unlike hydrometallurgical processes, high temperature (1400–1500 °C) pyrometallurgical processes can directly treat intact cells or entire modules with minimal pre-homogenization and concentration, although black mass is a possible option.[3] Pyrometallurgical processes can also tolerate a wider range of copper, cobalt, and nickel bearing raw materials, and the industrial hydrometallurgical Li-ion battery treatment has emerged only quite recently.[6] Pyrometallurgical processing is therefore expected to remain dominant despite the increasing hydrometallurgical black mass treatment capacity.[6] It is also noteworthy that the flowsheets used to refine pyrometallurgically produced battery metal alloys tend to be rather similar to the direct hydrometallurgical treatment of black mass,[7] given that both aim to separate cobalt, nickel, and copper from impurities.

Pyrometallurgical processing of lithium-ion batteries has been criticized primarily for high energy consumption, the direct carbon emissions from the combustion of organics and graphite, and the loss of particularly lithium to slag. The processes can, however, be largely autothermal particularly if the feed is high in aluminum, and the graphite anodes can also contribute to the reduction reactions in the process.[8,9] Lithium slagging can also be avoided by volatilizing it with a suitable flux and recovering it from the flue dust, a technology patented by Umicore.[10] The decomposition of organic compounds may, in some cases, also be considered an advantage since this enables the capture of hazardous fluoride compounds from the flue gas stream instead of having to treat fluoride-bearing wastewaters.

A significant challenge for recyclers is the heterogeneity of lithium-ion battery chemistries, and the trends in development have sometimes been difficult to predict. Lithium cobalt oxide (LCO, $LiCoO_2$), the first commercial cathode chemistry, is used in portable electronics but not in EVs due to the cost of cobalt.[11] Lithium nickel manganese cobalt oxide (NMC, $LiNi_xMn_yCo_{1-x-y}O_2$), where cobalt is partially substituted by nickel and manganese, is forecasted to continue dominating the EV market with increasingly high-nickel chemistries.[12] The only currently commercial cobalt-free cathode chemistry, lithium iron phosphate (LFP, $LiFePO_4$), has been gaining surprising momentum also outside of China despite its lower electrochemical performance.[13] Other entirely cobalt-free cathodes, such as lithium nickel manganese spinels ($LiNi_xMn_yO_4$) and manganese-based chemistries, may also breach the market in the future.[14] The forecasting is further complicated by the continued development of non-lithium-ion batteries, such as sodium-ion and lithium–sulfur,[15] which may likely require tailored recycling solutions due to their drastically different chemistries.

The environmental impacts of different recycling processes have received plenty of attention in the recent years using the standardized life cycle assessment (LCA) method.[16,17] Comparison of pyrometallurgical and hydrometallurgical approaches usually indicate that hydrometallurgical processing is more advantageous,[18–23] but Van Hoof *et al.*[7] concluded that hydrometallurgical black mass processing results in higher indirect or background emissions despite the lower direct emissions to air. Rajaeifar *et al.*[24] have also shown that pyrometallurgical processing can be made environmentally more competitive by adoption of changes to flowsheets, while Rinne *et al.*[25] and Cao *et al.*[18] have sought to lower the impacts of hydrometallurgical processes. A superficial comparison of generic processes by LCA does not typically provide enough information about their strengths or weaknesses, however. Both pyrometallurgical and hydrometallurgical treatment will be used industrially in the future, so it is necessary to look for opportunities to decrease the environmental impacts of recycling regardless of the type of process.

Given the importance of further process development, a detailed LCA was conducted to analyze the impacts of pyrometallurgical flowsheets in high resolution using process simulation for life cycle inventory gathering. The selected flowsheets were modelled using Metso's HSC Sim 10 software[21] to assess the effect of different process configurations and recently introduced technologies, such as lithium recovery by chloride volatilization. The results of the simulation were also evaluated with respect to the European Union's recovery targets to recognize the strengths and weaknesses of currently emerging pyrometallurgical battery processing pathways.

2. Materials and methods

The work follows the LCA framework outlined in ISO 14040:2006/A1:2020:en,[16] and consists of goal and scope definition, LCI analysis, life cycle impact assessment (LCIA), and interpretation stages. The LCI data was obtained by process simulation using HSC Sim 10 software,[26] and the battery composition and pre-treatment were modeled using Argonne National Laboratory-developed EverBatt tool.[27] LCIA was con-

Open Access Article. Published on 07 February 2025. Downloaded on 10/26/2025 6:04:00 AM.
This article is licensed under a Creative Commons Attribution 3.0 Unported Licence.

ducted with OpenLCA software v.2 [28] and background data was sourced from Ecoinvent 3.10 database.[29]

2.1. Goal and scope

The goal of this study is to assess the environmental impacts of Li-ion battery cell processing in Europe while reviewing the typical critique aimed against pyrometallurgical–hydrometallurgical treatment: energy intensity, direct emissions, and limited valuable recoveries. The study is prospective and considers some currently emerging technologies, such as pyrometallurgical lithium recovery[10] and the often overlooked aluminum separation during pre-treatment.[6] The pyrometallurgical and hydrometallurgical unit processes were simulated with HSC Sim 10 to obtain internally consistent and detailed mass and energy balances, which supports the goals of the study. The simulations were built with literature data, which also enables the transparent reporting of the LCI and the assumptions behind the data.

The functional unit (FU) of the study is input based: 1 metric tonne of spent battery cells entering the recycling process. The studied cell chemistries were lithium nickel manganese cobalt oxide ($LiNi_xMn_yCo_{1-x-y}O_2$) with two stoichiometries: the currently common NMC111, emerging NMC811, and the only commercial non-cobalt and nickel cathode, lithium iron phosphate ($LiFePO_4$, LFP). Substitution method was used to provide credits to recovered metals and metal salts at 1 : 1 ratio, which is reasonable given the recycled materials are functionally equivalent to primary metal compounds. Negative total impacts would therefore indicate that the benefits exceed the impacts of the recycling process, and positive total impacts would mean that recycling is more intensive than virgin raw material production.

European Commission-proposed Environmental Footprint, EF 3.0, method was used in the impact assessment. The included impact categories were acidification, climate change, eutrophication (freshwater, marine, terrestrial), human toxicity (carcinogenic and non-carcinogenic), ozone depletion, photochemical ozone creation, and abiotic depletion of minerals and metals. The optional stages in LCIA: normalization and weighing, were not conducted.

2.1.1. Feed materials. Pyrometallurgical battery processes can tolerate cells and modules as their feed, but the mechanical pre-treatment of the cells (*i.e.*, black mass route) may have some benefits, such as the possibility to recover aluminum and the decreasing problematic and corrosive fluoride entering the furnace. Although the benefits of aluminum recovery have already been established in some studies,[19,20] it may also be an important heat source in the pyrometallurgical process.[8] Therefore, the effect of pre-treatment on the heat and mass balance was investigated in two types of scenarios: pyrometallurgical processing with and without mechanical pre-treatment. The feeds were therefore either intact cells in the absence of pre-treatment, or black mass when black mass is implemented.

The study was conducted at cell-level with different cathode chemistries. NMC chemistries at various stoichiometries have emerged as the dominating cathode type particularly in Europe and the United States, but entirely cobalt and nickel-free LFP has gained momentum as a cheaper and safer alternative.[30] The cobalt in NMC has over time been increasingly substituted by nickel, which improves the electrochemical performance despite compromising stability, leading to the development of 532, 622, and 811 Ni–Mn–Co stoichiometries in the addition to the equimolar 111.[31,32] Although other cobalt-free and non-lithium chemistries are also emerging,[32] shifts in the market affect EOL recycling with a delay due to the long use time of the batteries. In this work, the currently prevailing NMC111, the emerging NMC811, and LFP were considered as raw materials.

The compositions of the feeds to the pyrometallurgical process were obtained from the EverBatt tool[27] and modified for HSC Sim 10. The compositions are presented in Table 1. NMC materials were represented in the simulation as stoichiometric mixtures of individual nickel, cobalt, and manganese oxides as seen in the table. Graphite and carbon black were included together as elemental carbon. If the polymers or plas-

Table 1 Battery waste feed material compositions (wt%) as used in the model (HSC Sim 10)

	Cells (%)			Black mass (%)		
	NMC111	NMC811	LFP	NMC111	NMC811	LFP
$LiCoO_2$	15.62	4.35	—	21.22	5.91	—
$LiNiO_2$	15.58	34.73	—	21.17	47.16	—
$LiMnO_2$	14.98	3.81	—	20.89	5.17	—
$LiFePO_4$	—	—	45.65	—	—	65.18
Carbon	26.66	29.98	23.50	35.66	40.73	33.55
Al	5.19	5.15	5.92	0.37	0.37	0.45
Cu	8.07	7.80	9.63	0.58	0.56	0.72
$LiPF_6$	1.67	1.74	1.87	0.00	0.00	0.00
PVDF	1.49	1.49	1.41	0.11	0.10	0.10
Dimethyl carbonate	4.23	4.34	4.68	0.00	0.00	0.00
Ethyl carbonate	5.22	5.36	5.78	0.00	0.00	0.00
PP plastic	0.85	0.80	1.06	0.00	0.00	0.00
PE plastic	0.18	0.17	0.23	0.00	0.00	0.00
PET plastic	0.26	0.28	0.27	0.00	0.00	0.00

Open Access Article. Published on 07 February 2025. Downloaded on 10/26/2025 6:04:00 AM.
This article is licensed under a Creative Commons Attribution 3.0 Unported Licence.

tics polyvinylidene fluoride (PVDF), polypropylene (PP), polyethylene (PE), or polyethylene terephthalate (PET), were not present in the database in their polymer form, their respective monomers were used instead.

2.1.2. System boundary and scenarios. The investigated system is depicted schematically in Fig. 1, and it consists of the processing of the cells starting either with mechanical pre-treatment (pre-treatment or *pt* scenarios) or pyrometallurgical treatment (direct pyrometallurgical, *dp* scenarios) and ends with the hydrometallurgical recovery of copper, nickel, cobalt, and lithium. The treatment of flue gases and the neutralization of aqueous effluents is also included in the foreground system, and solid wastes are presumed to be deposited to landfill without further stabilization. The wastewater is assumed to be discharged to freshwater after effluent treatment. The boundary omits infrastructure, as well as the transport and disassembly of battery packs, and the study was therefore conducted at cell-level.

The most significant waste or by-product from the process is pyrometallurgical slag, which consists of silica, alumina, lime, and minor quantities of other metal oxides. Slags from Li-ion battery processing are presumably suitable to be used as construction material, but the slag was treated as waste in this study and did not have any credits. No credits were assigned to separated non-metallic materials, such as anode, plastics, polymers, or electrolyte, either.

Three cathode chemistries and two process configurations amounted to a total of six scenarios as summarized in Table 2 along with the details of the technology and recovered metals. The process flowsheets are discussed in more detail in the subsequent section.

The process was scaled for 7000 tonnes of cells annually – the approximate capacities reported for two Li-ion battery focused pyrometallurgical processes, Umicore and Glencore,[6] assuming 8000 hours of annual operation. The scaling mainly affected the electricity consumption of hydrometallurgical units in this assessment and is therefore not a key consideration in the LCA, where the results are regardless normalized for the functional unit. Plant capacity would, however, need to be given more thought if economic evaluation was to be conducted since pyrometallurgical processing is CAPEX-intensive and the net profits are highly dependent on scale. Pre-treatment increases costs related to the recycling process but may potentially also streamline downstream processing and related costs. The economic feasibility therefore warrants its own detailed investigation.

Table 2 Summary of the investigated scenarios, *dp* referring to recycling process with no mechanical pretreatment and *pt* to recycling of black mass

Scenario name	Cell chemistry	Technology
dp-111	NMC111	Direct pyrometallurgical processing, no pre-treatment. Recovery of copper, nickel, cobalt, and lithium.
dp-811	NMC811	
dp-LFP	LFP	
pt-111	NMC111	Processing of pre-treated black mass. Recovery of copper, aluminum, nickel, cobalt, and lithium.
pt-811	NMC811	
pt-LFP	LFP	

2.2. Process description

As discussed earlier, some pyrometallurgical, or more accurately pyrometallurgical–hydrometallurgical processing can accept a wide array of nickel and cobalt-containing feeds, such as modules, cells, black mass, or concentrates.[8] A model for

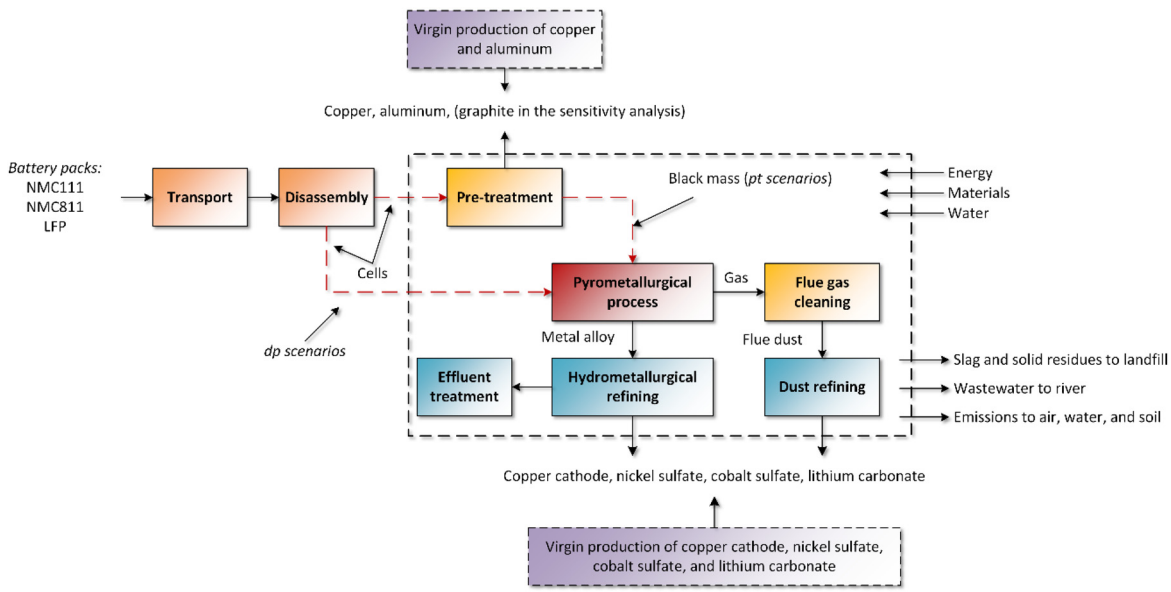

Fig. 1 System boundaries in the study shown with dashed lines. The foreground system is with a transparent background and the compared product systems (primary metal production routes) with lavender. The alternative direct pyrometallurgical *dp* and pyrometallurgical with pre-treatment *pt* scenarios are highlighted with red arrows.

Open Access Article. Published on 07 February 2025. Downloaded on 10/26/2025 6:04:00 AM.
This article is licensed under a Creative Commons Attribution 3.0 Unported Licence.

the mechanical pre-treatment was directly adopted from the EverBatt tool.[27] The pyrometallurgical reduction smelting process was modeled mainly based on the information of the Umicore process operating in Belgium[8] with the addition of lithium fuming to recover it from the flue dust.[10] A generic sulfuric acid-based hydrometallurgical flowsheet was drawn for the refining of pyrometallurgical copper–nickel–cobalt-bearing alloys. The process consists of state-of-the-art technologies such as sulfuric acid leaching, solvent extraction (SX), electrowinning (EW), and crystallization. The simplified flowsheet without solid/liquid separation units is presented in Fig. 2, and in more detail in Fig. S1–S3.† Process parameters used in the simulation are summarized in Tables S1 and S2 in the ESI.†

The pre-treatment of lithium-ion batteries is complex, and many different technologies can be used for the comminution and liberation of different material fractions, consisting of possible discharging or inactivation, comminution, sometimes thermal treatment, classification, and separation processes.[5] In the default EverBatt process, the cells are first shredded, after which the polymers and electrolyte are pyrolyzed at medium temperature while avoiding graphite combustion. The metals: iron, copper, and aluminum, are then separated from the electrode powders (black mass). In industrial operation, it has presumably been more common that the mixture of current collector scrap is sent to copper smelters – without aluminum and copper separation – allowing copper to be recycled while losing aluminum.[7] Some relatively recent European black mass producers, such as Fortum and Northvolt, appear to recover aluminum,[33,34] so this was included in the LCI model.

Pre-treatment processes themselves are complex combinations of several optional unit processes for the liberation and separation of material fractions, and no identical process chains exist. The separation of active material powder from current collector foils is typically achieved by size classification, such as sieving.[5] The process suffers from poor selectivity due to the polymeric binder, usually polyvinylidene fluoride (PVDF), which is sometimes decomposed by thermal pre-treatment to improve liberation, although this may promote aluminum oxidation and the loss of electrolyte as trade-offs.[35] A challenge of the process is to maximize recovery while minimizing impurities in the black mass, since the use of smaller sieve size leads to higher active material losses while also producing purer black mass. Circular design by the use of water-soluble binders has been recommended in literature to simplify recycling routes.[35]

In reduction smelting, the valuables are separated into molten metal, slag, and gas phases at high temperatures. While the processes operate with similar principles, different smelting technologies, such as rotary hearth furnace, electric arc furnace, shaft furnace, are used by industrial operators.[6] The model assumes an Umicore-type shaft furnace process due to the best data availability, but the results presumably apply reasonably well for other similarly operated pyrometallurgical–hydrometallurgical processes.

The shaft furnace has three vertical temperature zones: pre-heating (<300 °C), pyrolysis (~700 °C), and reaction zone (1200–1450 °C).[36] The electrolyte evaporates in the pre-heating zone, plastics pyrolyze in the pyrolyzing zone, and most of the reduction reactions occur in the reaction zone.[37] Reducing power is supplied by metallic aluminum and carbon, either in the form of graphite or coke, and the most important reactions are given by reactions (1) and (2), where Me is nickel, cobalt, or to a lesser degree manganese.[37] Metals with higher oxygen

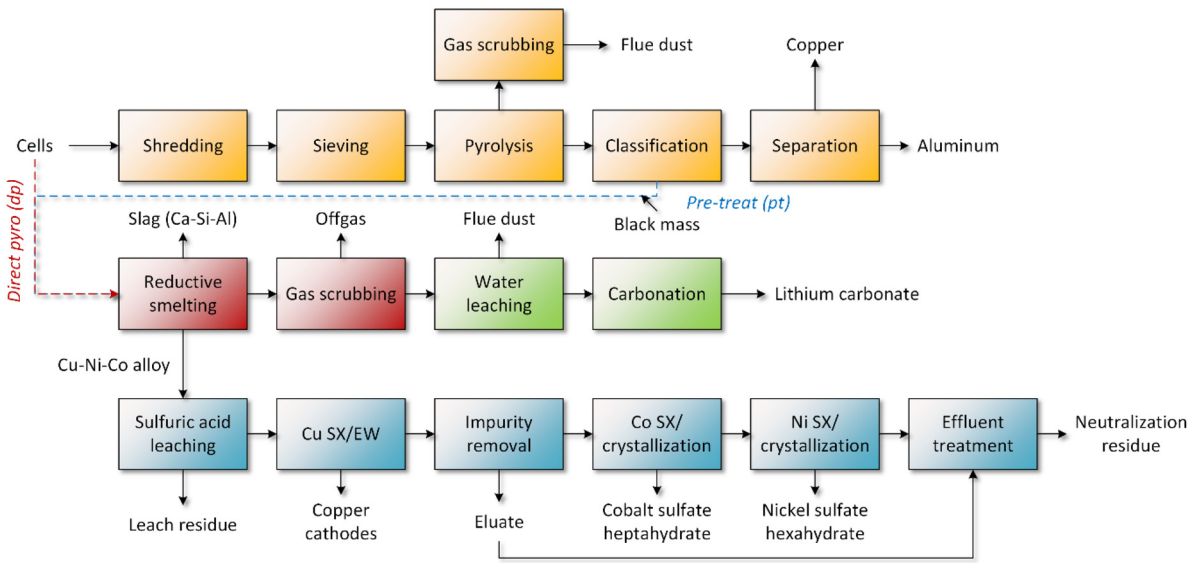

Fig. 2 Simplified process flowsheet in scenarios *dp* (red, green, and blue units) and *pt* (yellow, red, green, and blue units). Units are classified into pre-treatment (yellow), pyrometallurgical processing (red), flue dust treatment for lithium recovery (green), and hydrometallurgical alloy refining (blue).

Open Access Article. Published on 07 February 2025. Downloaded on 10/26/2025 6:04:00 AM. This article is licensed under a Creative Commons Attribution 3.0 Unported Licence.

affinity than nickel and cobalt (*e.g.*, lithium, manganese, aluminum, silicon, calcium) mainly dissolve in the slag as oxides. Iron's thermodynamic behavior is close to cobalt, so it partially reports to the metallic phase.

$$2LiMeO_2 + 2Al \rightarrow Li_2O(l) + 2Me(l) + Al_2O_3(l) \quad (1)$$

$$2LiMeO_2 + 3C \rightarrow Li_2O(l) + 2Me(l) + 3CO(g) \quad (2)$$

The possibility for recovering lithium from slag has been discussed, but lithium is typically in the slag in the form of silica and alumina gel forming aluminosilicates, which makes filtration of the leach residues difficult.[38,39] These issues can be added by roasting pre-treatment where lithium-bearing minerals are converted to water-soluble phases.[38,40] Lithium slagging can also be minimized by the addition of a suitable flux, such as calcium chloride ($CaCl_2$). Instead of reporting to slag as an oxide, lithium forms volatile lithium chloride (LiCl), which evaporates and can be recovered from the captured flue dust. In Umicore's patent, 20% stoichiometric excess of chloride volatilized 96% of lithium.[10] The volatilization of lithium from the slag is described by reaction (3).

$$Li_2O(slag) + CaCl_2(flux) \rightarrow LiCl(g) + CaO(slag) \quad (3)$$

The release of hazardous halogenated compounds is avoided by gas cleaning. Cheret and Santén[8] describe a method, where a plasma torch is used to heat the exit gas (250–700 °C) to 1150 °C. Fluoride is then captured in the combustion chamber by injecting calcium oxide (or zinc oxide), binding fluoride as insoluble calcium fluoride (CaF_2), and the gas is cooled rapidly to 300 °C to prevent the re-formation of halogen compounds. The subsequent gas cleaning consists of cooling and de-dusting systems, such as evaporating cooling, baghouse filter, and wet gas cleaning units. The flue dust containing lithium chloride is collected and treated hydrometallurgically for lithium recovery by water leaching and carbonation. Calcium, the main water-soluble metallic impurity in the dust, can be removed from the solution by an additional carbonation step.[41] The de-dusted gas rich in carbon dioxide is released to the atmosphere.

The flowsheet for alloy refining was designed to reflect a very generic process copper/nickel/cobalt/(iron/manganese) separation process consisting of sulfuric acid leaching, copper recovery as cathodes, and nickel and cobalt recovery as hydrated sulfates ($CoSO_4{\cdot}7H_2O$ and $NiSO_4{\cdot}6H_2O$). The metals are separated by stepwise SX: first copper followed by impurities, cobalt, and nickel in respective order. Many organic extractants and flowsheets may be applicable, so LIX-type reagents were selected for copper,[42] D2EHPA for the impurities,[43,44] and Cyanex 272 to separate cobalt from nickel.[43] Nickel is finally extracted with D2EHPA or Versatic 10. All circuits were presumed to be operated counter-currently and in sulfuric acid media using sodium hydroxide as neutralizing agent. Copper was recovered from the purified solution as metallic cathodes by EW, while cobalt and nickel were assumed to be recovered as heptahydrate and hexahydrate sulfate salts by generic evaporative crystallization. The impurity effluents and bleed solutions were treated by lime neutralization to remove metals from the solution.

2.3. Inventory modeling

The life cycle inventories were modeled in two ways: pre-treatment by the EverBatt model, and extractive metallurgy by HSC Sim 10. Background data for the input chemicals and energy sources were obtained from ecoinvent 3.10.

The used elementary flows, background datasets, and other details are available in the ESI,† along with the assumptions for electricity modeling (Tables S4–S6†). A forecast for European average electricity production in year 2030[45] was used to model the electricity mix of the foreground process. The forecast predicts 59% of all EU's electricity generation to be sourced from renewables and 17% from nuclear fission.

The material and energy inputs to the process are presented in Table 3 for the entire process chain consisting of the optional pre-treatment, pyrometallurgical processing, flue dust refining, and hydrometallurgical alloy refining. In addition to silica and limestone fluxes, granulated blast furnace slag (40% silica, 35% calcium oxide, 10% alumina, 15% iron oxide) was fed to the furnace as a slag former.[8]

The aggregated outputs: products, waste, and emissions to air and water are provided in Table 4. Aluminum is recovered only by pre-treatment (*pt* scenarios), while copper can be recovered either entirely pyro-hydrometallurgically or by a combination of pre-treatment and extractive metallurgy.

3. Results and discussion

The results consist of observations made in the process simulation and the LCIA and their interpretation.

3.1. Simulation insights

The simulation was used to critically assess particularly the valuable recoveries and the heat balance of the process, which may also affect the LCI and therefore the LCIA results.

3.1.1. Recoveries. The EU's Battery Regulation 2023/1542[46] imposes gradually increasing recovery target for total battery weight as well as element-specific targets for lithium, cobalt, nickel, and copper. By 2031, the goals are 70% total battery weight, and 95% recovered nickel, cobalt, and copper, and 70% lithium. The results are illustrated in Fig. 3 with respect to the targets. Although aluminum recovery is not shown in the Fig. 3, it contributes to battery weight recoveries in *pt-111*, *pt-811*, and *pt-LFP* scenarios, where 90% aluminum is presumed to be recovered. The assumptions for the estimation of battery weight recovery are provided in Section S1.5 of the ESI,† but it was assumed that the cells comprise ~60% of battery weight and the pack materials are recovered. The results are tabulated together with the recoverable cell weight in Table S8.† Cathode oxygen was excluded from the calculations as non-recoverable mass.

The 70% weight recovery target was not reached in any scenario as seen in Fig. 3, although *pt-811* came close at 66%.

Open Access Article. Published on 07 February 2025. Downloaded on 10/26/2025 6:04:00 AM.
This article is licensed under a Creative Commons Attribution 3.0 Unported Licence.

Table 3 Material and energy inputs to the recycling process per functional unit (FU, 1 t battery cells)

Inflows	*dp-111*	*dp-811*	*dp-LFP*	*pt-111*	*pt-811*	*pt-LFP*	Unit/FU
Cells	1.00	1.00	1.00	1.00	1.00	1.00	t
Electricity	1776.83	1780.89	1217.94	924.26	955.75	651.67	MJ
Diesel	—	—	—	600.00	600.00	600.00	MJ
Heat, natural gas	4604.07	4932.78	12 946.93	5193.64	5638.23	7501.56	MJ
Heat, steam	4622.39	5331.25	74.12	3222.65	3596.52	51.32	MJ
Metallurgical coke	0.00	0.00	0.38	0.00	0.00	0.14	t
Air, compressed	3.92	4.28	10.90	2.81	3.20	4.66	t
Oxygen, liquid	0.23	0.28	0.08	0.16	0.21	0.00	t
Nitrogen, liquid	—	—	—	0.05	0.05	0.05	t
Water	14.97	11.81	8.53	11.34	13.06	4.43	t
Silica sand	0.67	0.49	1.86	0.35	0.27	1.38	t
Limestone ($CaCO_3$)	0.50	0.25	0.05	0.03	0.00	1.37	t
Blast furnace slag	0.00	0.41	0.93	0.07	0.53	0.69	t
Calcium chloride	0.33	0.30	0.20	0.31	0.28	0.18	t
Lime (CaO)	0.08	0.10	0.06	0.02	0.06	0.02	t
Soda ash	0.30	0.28	0.18	0.28	0.25	0.17	t
Sulfuric acid	1.13	1.30	0.47	0.72	0.88	0.00	t
Caustic soda	0.64	0.71	0.34	0.58	0.70	0.05	t
Kerosene	0.41	0.47	0.11	0.28	0.34	0.01	t
Organic chemicals	0.18	0.21	0.08	0.12	0.15	0.01	t

Table 4 Products, waste, and emissions from the entire process

Outflows	*dp-111*	*dp-811*	*dp-LFP*	*pt-111*	*pt-811*	*pt-LFP*	Unit/FU
Product: aluminum	—	—	—	46.73	46.37	53.51	kg
Product: copper	76.10	73.51	90.11	76.47	73.87	90.61	kg
Product: cobalt sulfate	230.28	63.90	—	218.40	60.15	—	kg
Product: nickel sulfate	235.32	531.42	—	224.88	506.34	—	kg
Product: lithium carbonate	165.33	152.38	101.22	155.66	141.95	93.27	kg
Waste: solid slag	1.34	1.31	4.46	0.95	0.96	3.30	t
Waste: wastewater	7.70	8.75	6.35	6.00	6.84	1.42	t
Waste: solid residues	173.73	253.81	108.45	318.27	337.75	221.26	kg
Emissions: PM (>2.5 μm, <10 μm)	0.06	0.05	0.04	0.05	0.04	0.03	kg
Emissions: carbon dioxide to air	1.40	1.41	2.69	1.19	1.25	1.95	t
Emissions: fluoride to freshwater	0.02	0.02	0.02	0.02	0.01	0.01	kg
Emissions: chloride to freshwater	208.32	192.36	129.33	195.13	177.98	116.95	kg
Emissions: copper to freshwater	15.48	16.39	24.73	0.70	0.68	0.97	g
Emissions: nickel to freshwater	36.02	53.12	—	28.79	44.00	—	g
Emissions: cobalt to freshwater	10.04	3.06	—	10.61	2.96	—	g

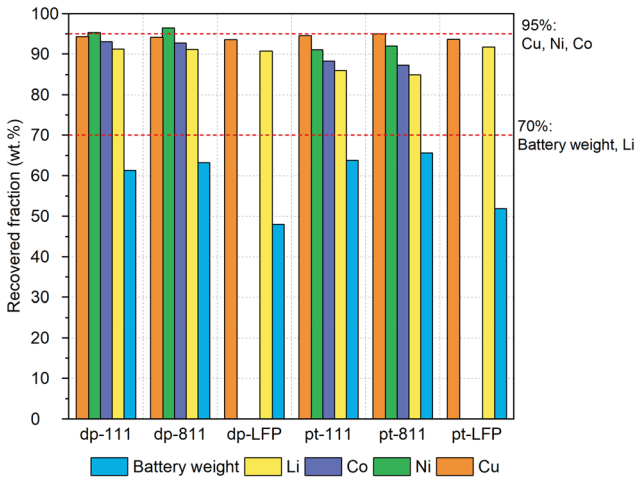

Fig. 3 Recoveries of battery weight and the valuables with respect to the EU Battery Regulation 2031 targets (red dashed lines).[46]

The used cell composition was quite low in aluminum (5–6%), so the goal in the case of *pt-111* (64%) and *pt-811* may be reached only through variability in the feedstock without changes in the process. The optimization of lithium, copper, cobalt, and nickel recovery in *dp* process is very unlikely to close the gap due to the already high recoveries, so the implementation of pre-treatment appears to be necessary for the target. This alone, however, is not enough for LFP, since the weight recovery for *pt-LFP* was only 52%, suggesting that LFP would ideally be treated in other types of processes. Manganese was not recovered, so its reclamation remains an option in the process to improve the overall recoveries by a small margin.

The recoveries of individual elements reached the targets consistently only for lithium (all scenarios >85%), but the target for copper in both *dp* (94%) and *pt* (93–95%) scenarios should realistically be attainable. The 95% goal for nickel is reached in direct cell smelting (*dp-111*: 95% and *dp-811*: 96%), but not in combination with pre-treatment (*pt-111*: 91% and

Open Access Article. Published on 07 February 2025. Downloaded on 10/26/2025 6:04:00 AM.
This article is licensed under a Creative Commons Attribution 3.0 Unported Licence.

pt-811: 92%) due to the active material losses to other metallic fractions (assumed 5% to copper–aluminum streams). According to the patent,[8] the smelting losses of nickel are 1–2%, but the very high solubility of nickel sulfate in aqueous solution causes some losses in the hydrometallurgical circuit which are likely preventable by process optimization. The 95% target is more challenging for cobalt (*dp-111* 93%, *dp-811* 93%, *pt-111* 87%, *pt-811* 88%) due to its higher affinity to slag (3–5% losses in reducing smelting). Improving cobalt recovery would therefore require more reductive atmosphere in the furnace, which would also lead to a higher amount of iron and likely manganese reducing and dissolving in the alloy.

The losses in pre-treatment (5% active materials) were assumed constant, but they realistically depend on the selectivity of the used mechanical separation and classification units and are affected by several factors. The binder material has been recognized as one of the more significant challenges for material separation in pre-treatment,[35] so finding effective measures to remove the polymeric materials while avoiding downstream problems by altering the chemistry and morphology of metallic and black mass components is necessary. In the longer term, it is worth considering to replace the currently widely used PVDF materials with water soluble or otherwise more circular alternatives.

Considering graphite makes up approximately 20–30% of the cell weight, its valorization would significantly boost the overall recycling efficiency. This was studied in the sensitivity analysis, and the numerical values are reported in Table S8.† In the analysis, it was assumed that 90% of graphite would be separated to its own stream during pre-treatment and therefore would not enter the smelting process as a reducing agent. With the implementation of graphite recovery, the 70% battery weight recovery target was reached for NMC111 (80%) and 811 (84%), and it is also within reach for LFP (67%). This study did not consider manganese, which mostly reports to the slag and the rest to the alloy phase. Considering that manganese recovery is not mandated by regulation and it is not currently considered as a costly metal, the development of robust technologies for its extraction may be challenging.

Despite the uncertainties, the analysis suggests that the EU Battery Regulation goals[46] are highly ambitious and difficult to reach even for the metals that already have well established recovery routes. The addition of further process steps, such as pre-treatment, is typically necessary to recover more individual materials and/or overall battery weight, but this also leads to cumulative valuable losses if the separation processes are not adequately selective. The separation of lithium by high temperature volatilization was an exception to this as a highly selective process, since no other valuable metals in Li-ion batteries form volatile chlorides, and no additional losses therefore occurred.

3.1.2. Heat balance. The claim repeated in scientific literature "pyrometallurgical processing is energy intensive" was investigated with the process simulation. Opposite to commonly used claim, the suggested that the reducing smelting process can be autothermal in the case of all NMC scenarios with the studied parameters. The results showed that heat needed for the process was supplied by the exothermal reactions of graphite and aluminum oxidation. There were, however, several sources of uncertainty, such as the effect of the amount of slag and heat losses from the furnace. Also, opposite to NMC waste batteries, additional heat was needed in the LFP scenarios most likely due to the high amount of slag. LFP batteries only have copper and iron to contribute to alloy mass, so the slag/alloy ratio was not controlled. In practice, this indicates that the treatment of LFP batteries alone requires external heat to maintain the slag above liquidus temperature. The heat losses in the furnace were assumed 10% of the input enthalpy: a preliminary assessment with varying heat losses (0–20%) did not show any changes in the conclusions, *i.e.*, the process was autothermal for NMC but not LFP materials, and a more rigorous calculation procedure was therefore deemed unnecessary.

Although the furnace itself operated autothermally in NMC scenarios, the pre-heating of air and the combustion of flue gases required external heat, which was modeled with natural gas in the LCI. Pre-treatment in each of the *pt* scenarios consumed 2000 MJ of natural gas for 1 tonne of cells, and the rest of the consumed gas is relative to the volume of flue gas. The processing of cells (*dp*) produced more gas than black mass, while the treatment of LFP materials produced more than NMC, and NMC811 stoichiometry slightly more than NMC111.

The hydrometallurgical units were assumed to be heated with steam if necessary. It was presumed that the lithium-bearing dust is processed at 80 °C, which consumed a small amount of external heat. Most of the steam required in the processing of NMC-based alloys was consumed in the crystallization of nickel and cobalt sulfates, however, which explains the discrepancy between LFP and NMC scenarios (Table 3). The solubility of nickel sulfate in sulfuric acid solutions was higher than cobalt sulfate,[47,48] leading to higher steam consumption for NMC811 than NMC111.

It should be observed that no waste heat recovery was implemented in the gas treatment line, so all the steam in the LCI was modeled with an external feed. The inclusion of heat recovery can minimize if not completely avoid external steam consumption. The significance of this on the environmental impacts could, however, be evaluated with the contribution analyses in Section 3.3. Overall, graphite and aluminum alone can potentially supply all the reducing power and heat needed in the process for typical feed mixtures consisting largely of nickel and cobalt-bearing batteries.

3.2. Impact assessment

The results of the impact assessment, consisting of the process itself and the recovery credits, are shown in Fig. 4 and 5. Fig. 4 shows the acidification (AC), abiotic depletion (AD), climate change (CC) and eutrophication (freshwater, marine, and terrestrial; EUf, EUm, EUt), while Fig. 5 presents human toxicity (cancer and non-cancer; HTc and HTn), ozone depletion (OD), and photochemical ozone formation (POF). The results highlight, overall, that the net impacts accounting

Open Access Article. Published on 07 February 2025. Downloaded on 10/26/2025 6:04:00 AM.
This article is licensed under a Creative Commons Attribution 3.0 Unported Licence.

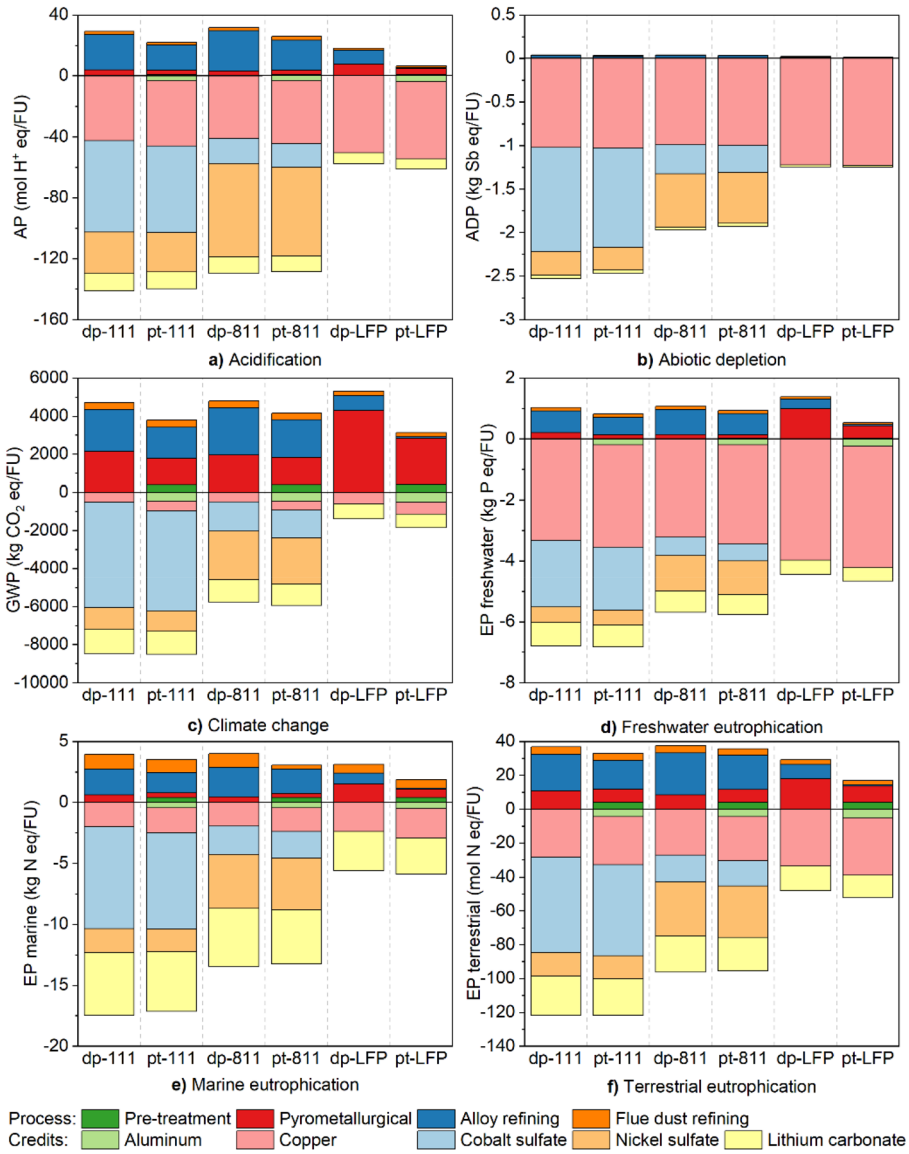

Fig. 4 Impact assessment of the scenarios showing the contribution of process stages and credits, "pyrometallurgical" consists of reduction smelting and flue gas cleaning, "alloy refining" of the stages from alloy leaching to the recovery of copper, nickel, and cobalt, and "dust refining" consists of lithium leaching and precipitation. (a) acidification, AC (b) abiotic depletion, AD (c) Climate change, CC (d) freshwater eutrophication, EUf (e) marine eutrophication, EUm (f) terrestrial eutrophication, EUt.

both credits and process impacts were negative, *i.e.*, recycling leads to reduced environmental impacts compared to primary production with some exceptions outlined below.

The assigned recycling credits represent the environmental intensity of the virgin metal production routes and were therefore not equal between the different chemistries, but some uncertainty may also arise from the underlying characterization model in the LCIA method particularly in the case of toxicity and abiotic depletion. The primary route for cobalt sulfate production, for instance, is more intensive (per 1 kg $CoSO_4$) than nickel sulfate, so the credits for NMC111 were higher than NMC811. In contrast, the differences in processing impacts, *e.g.*, the positive bars, were negligible, which would imply that the recycling of NMC111 leads to higher net environmental impact reduction than NMC811. The processing impacts were more challenging to mitigate for LFP due to the only recovered metals being copper, lithium, and possibly aluminum. For the aforementioned reasons, all impact categories for NMC111 were net negative in both scenarios, but some positive values were recognized for NMC811 and LFP. Both direct pyrometallurgical (*dp*) and pre-treatment (*pt*) scenarios of NMC811 treatment were positive in terms of ozone depletion, +64 and 67% respectively. Pre-treatment mitigated the impacts more effectively for LFP, and the only net positive for *pt-LFP* was CC (+281%), while *dp-LFP* was positive in terms of CC (+69%), HTc (+84%), OD (+422%), and POF (+15%).

Open Access Article. Published on 07 February 2025. Downloaded on 10/26/2025 6:04:00 AM.
This article is licensed under a Creative Commons Attribution 3.0 Unported Licence.

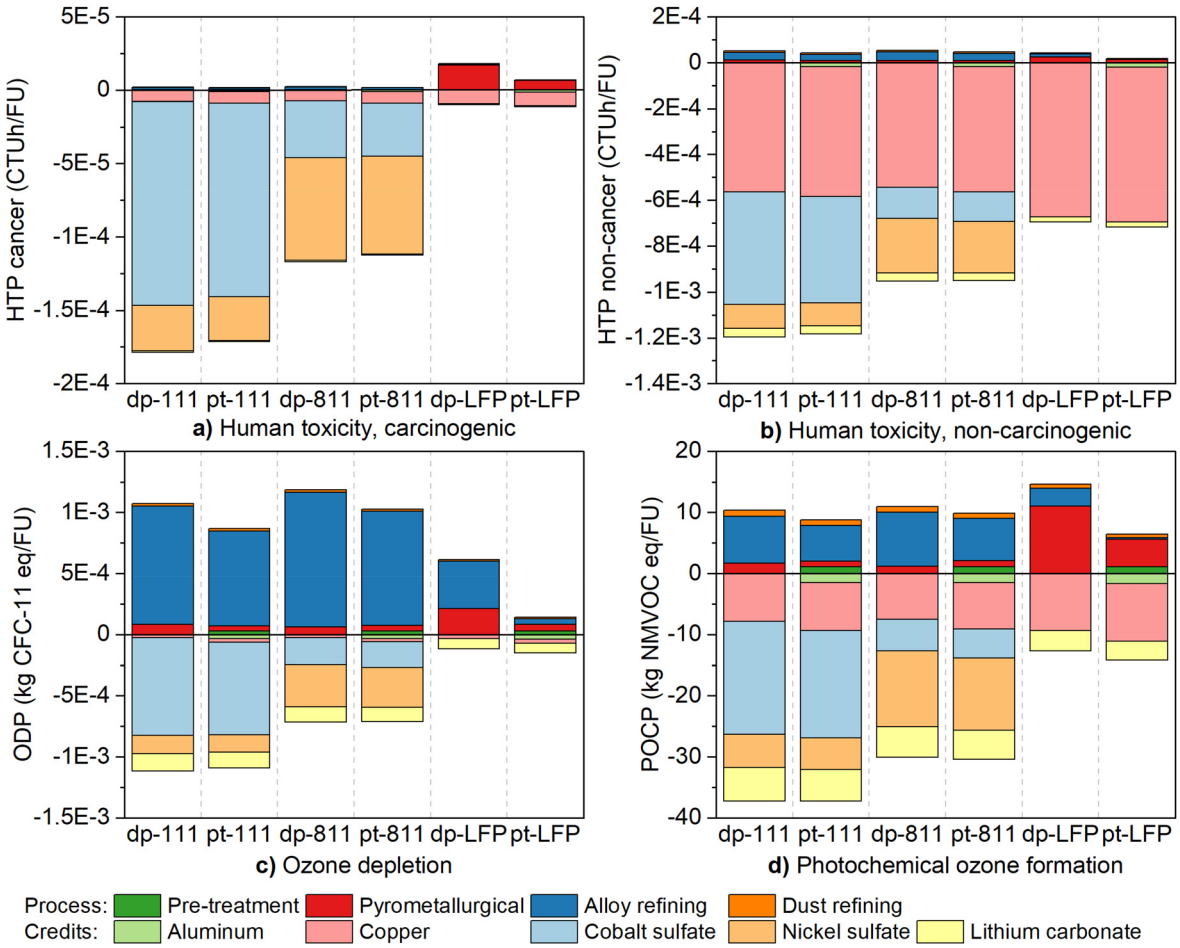

Fig. 5 Impact assessment of the scenarios. (a) Carcinogenic human toxicity, HTc (b) non-carcinogenic human toxicity, HTn. (d) Ozone depletion, OD (e) photochemical ozone formation, POF.

The key finding from Fig. 4 and 5 was that the implementation of pre-treatment lead to reduced recycling process impacts for all chemistries, especially for LFP. The reduction was approximately 10–25% for NMC111, 5–20% for NMC811, and 40–80% for LFP. Although the benefit of pre-treatment has been previously discussed to be due to aluminum reclamation,[24,49,50] the credits for aluminum in this study could not repeat the effect. Aluminum recovery was significant perhaps for LFP, which has low amounts of recoverable elements in the battery structure. The main factor explaining the lower impacts when using preprocessing steps for the battery waste therefore appeared to be the lower volume of raw material entering the pyrometallurgical recycling process and consequently the following hydrometallurgical refining. The relatively low amount of aluminum in the cells (5.2% both NMC, 5.9% LFP) may explain this and therefore underestimate the potential aluminum credits, but it can nevertheless be established that pre-treatment also carries other benefits as well by decreasing the amount of material that needs to be subjected to intensive treatment and lowering the amount of corrosive fluoride.

As seen in the two figures, the process was roughly divided into pre-treatment, pyrometallurgical, hydrometallurgical alloy refining, and hydrometallurgical dust stages. The contribution profiles were similar for the *dp* and *pt* scenarios of both NMC chemistries: *e.g.*, alloy refining is the dominating "hotspot" for NMC processing (for example, CC *dp-111* 46.1%, *pt-111* 51.9%; *dp-811* 43.8%, *pt-811* 47.7%). The implementation of pre-treatment decreased the overall contribution of alloy refining in *pt-111* and *pt-811* by a few percentages from the respective *dp* scenarios, while pre-treatment itself was a relatively minor part of the process (0.5–10%), further supporting the recommendation for the implementation of pre-treatment processes. The impact of lithium recovery was fairly constant between the scenarios and unaffected by process configuration aside from *dp-LFP*, where the contribution was higher than the other scenarios due to the overall lower processing impacts. The most significant impact categories in terms of lithium refining were marine eutrophication (~25–30%, *pt-LFP* 36%) and resource depletion (~16–20%, *pt-LFP* 37%). Contribution analysis was used to evaluate further why the hydrometallurgical stages were so highly represented in the process, Section 3.3.

Open Access Article. Published on 07 February 2025. Downloaded on 10/26/2025 6:04:00 AM. This article is licensed under a Creative Commons Attribution 3.0 Unported Licence.

The stage contributions of LFP were different from NMC due to the overall low amount of metal alloy entering the hydrometallurgical refining process and the need for external carbon in the pyrometallurgical stages. The impacts of pyrometallurgical processing therefore exceeded the alloy refining stages consistently in *pt-LFP* scenario (38–96% pyrometallurgical; 1–34% alloy refining), and *dp-LFP* (49–96% pyrometallurgical; 3–35% alloy refining) with the exception of acidification (42% pyrometallurgical; 51% alloy refining), ozone depletion (35% and 63%), and abiotic depletion (33% and 48%).

The net benefits of the process were dependent on credits from the recovery of individual valuables, so the recoveries of said valuables affects the conclusions and should therefore be assessed. Between the *dp* and *pt* scenarios for NMC, the recoveries of nickel, cobalt, and lithium decreased ~4–5% due to pre-treatment losses. However, the effect on the individual credits (Fig. 4 and 5) was not substantial and the credits were directly proportional to the recoveries, *i.e.*, the credit for cobalt sulfate was 5% smaller in *pt* than the corresponding *dp* scenario. Assuming that the recoveries are overpredicted, a decrease of a few percentages does not appear to affect the net impacts to change the overall conclusions except by turning the ozone depletion to net positive and decrease the benefits in other impact categories, although higher valuable losses would nearly inevitably make it impossible to reach the Regulation goals.

Although the model was only run with NMC and LFP chemistries, the results provide some insights into the recycling of other battery chemistries as well. Cobalt, copper, and nickel provide most of the recycling credits by being efficiently recovered in the process. Therefore, the substitution of particularly cobalt with other elements leads to lower overall benefits. Since the primary production of cobalt was more intensive than the substituting nickel. Manganese-rich chemistries, such as the potentially emerging lithium nickel manganese spinel, would pose problems due to the lack of recovery route for manganese, although nickel can be effectively reclaimed from the batteries. Since benefits were observed for LFP in a number of impact categories, the processing of nickel–manganese cathodes in the process would nevertheless be more advantageous than harmful. The limitations of recycling industry and its unit processes should, however, be taken into consideration in the development of battery chemistries and design.

3.3. Contribution analysis

Contribution analysis of the scenarios (Fig. 6) was conducted to aid the interpretation of the results. The analysis is for the whole process and not differentiated between process stages, but they are presented separately in the ESI.† Electricity, heat (steam, natural gas), and water are consumed in all process stages, lime and the grouped "air, oxygen, and nitrogen", in all except dust refining. Foreground emissions were produced in pre-treatment and pyrometallurgical processing, while the metal emissions to water had no impacts in EF 3.0. Diesel was unique to pre-treatment, coke and calcium chloride to pyrometallurgical processing; sulfuric acid, caustic soda, and organics to alloy refining, and soda to dust refining.

The analyses of NMC scenarios appeared quite similar and seem to explain why the hydrometallurgical alloy refining is so overrepresented in the process chain. Caustic soda and organics were the hotspots of the process along with sulfuric acid for acidification. Energy inputs: diesel, natural gas, steam, (coke), and electricity, accounted to approximately 2–20% of the impacts between all NMC scenarios but was, overall, slightly higher in *pt* scenarios due to diesel. If direct carbon dioxide emissions are included to energy inputs, the share of energy for CC increases to ~50%, with the foreground carbon dioxide accounting to 29–31% in all the NMC scenarios.

Unlike NMC, the processing of LFP consumed coke as a reducing agent, and the contribution of energy sources and fuels was more significant aside from AD, which was in a similar scale to NMC (5% *dp*, 4% *pt*). Coke consumption dominated especially Ef (60% both *dp* and *pt*), HTn (94% *dp*, 93% *pt*), and POF (67% *dp*, 71% *pt*), and also resulted in high foreground greenhouse gas emissions (51% *dp*, 69% *pt*). The model likely overestimated the needed amount of coke: much of it was consumed in simply maintaining the furnace temperature, which can also be achieved by other carbonaceous fuels or the use of electricity in certain types of furnaces. The pyrometallurgical processing of LFP materials has many challenges, including high volume of phosphorus-rich slag, low overall recoveries, and most likely low economic feasibility, so the environmental impact results are nevertheless indicative.

In addition to energy sources, the pyrometallurgical process stage consumed air, cooling water, calcium chloride for lithium volatilization, and slag formers. Even as an aggregate with oxygen (for alloy leaching) and nitrogen (for pre-treatment), air was associated with quite limited impacts, <5% apart from EUf, 10–15%. LFP treatment required far more slag fluxes to dilute the phosphorus and iron, but even in then, the impacts from slag formers were moderate (*dp-LFP*, AC: 5.1%, AD: 1.4%, CC: 2.2%, EUf: 1.4%, EUm: 8.2%, EUt: 9.8%, HTc: 0.3%, HTn: 3.1%, OD: 2.3%, POF: 5.3%).

Organics and caustic soda were identified as the hotspots in NMC processing but not LFP since three of the four the SX circuits were not needed in LFP processing. The two chemicals alone would suggest that SX is one of the high impact areas of the process, as caustic soda is used as the neutralizing chemical specifically in SX. This is not unexpected, given that SX units have previously been observed to dominate the impacts of hydrometallurgical black mass processing, and possible countermeasures and management of uncertainty have been discussed by Rinne *et al.*[25] The organic was modeled in the LCI as a mix of kerosene and unspecified organic chemical, so the results could be different with more specific data of the extractants. Regardless, the degradation rate of the organics would need to be experimentally confirmed, and the actual consumption of organics can only be determined in industrial scale due to factors such as crud formation given that SX is a highly sensitive process.

 This journal is © The Royal Society of Chemistry 2025

Open Access Article. Published on 07 February 2025. Downloaded on 10/26/2025 6:04:00 AM.
This article is licensed under a Creative Commons Attribution 3.0 Unported Licence.

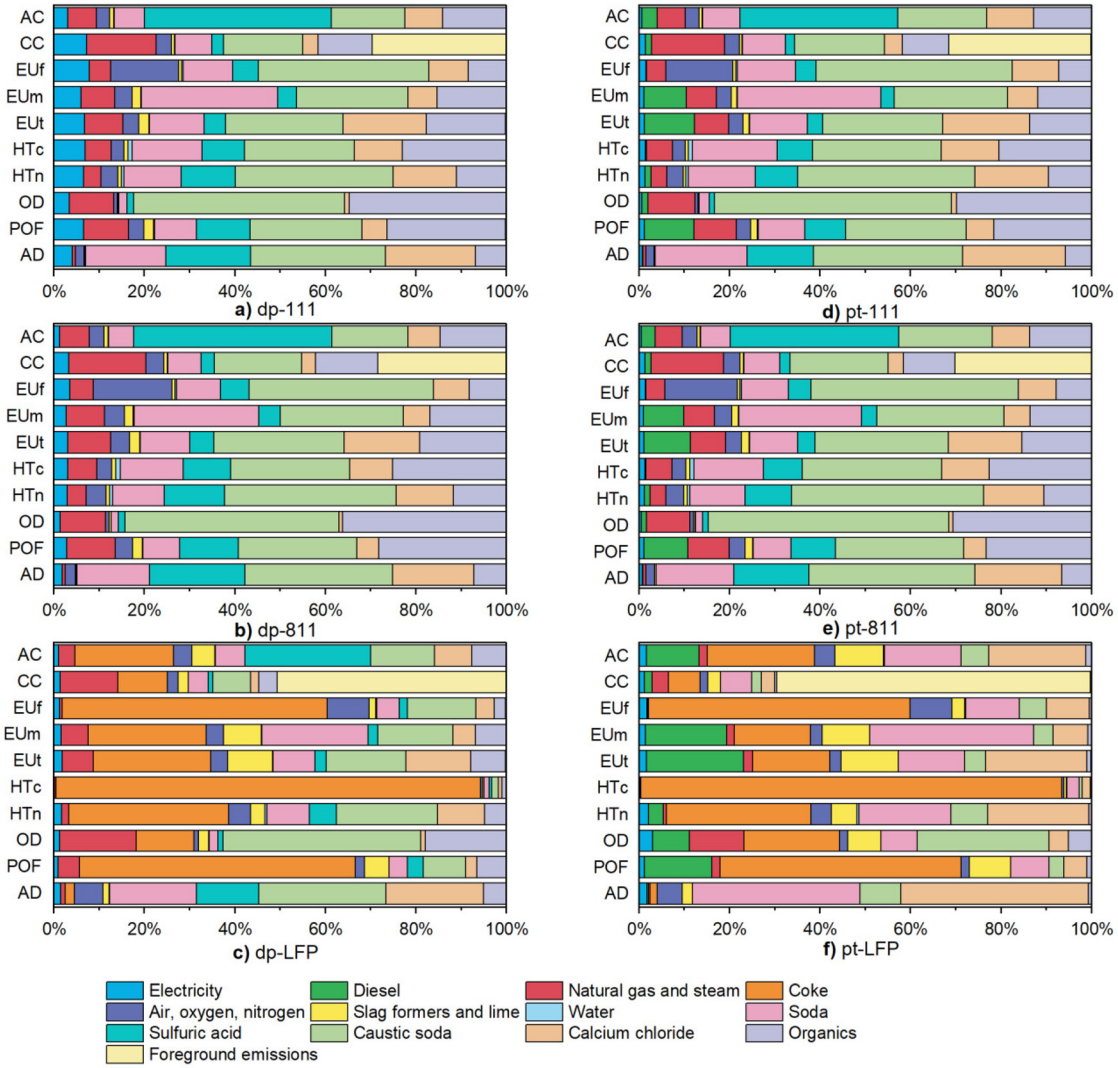

Fig. 6 Relative contributions of background and foreground processes to the impacts, where "slag formers" refers to silica sand, limestone, and blast furnace slag fluxes.

Calcium chloride was the only seemingly significant non-energy input to the furnace particularly in terms of terrestrial EP and AD, ~20% across the scenarios. The amount of calcium chloride was only relative to the amount of lithium and therefore quite certain. In the impact analysis (Fig. 4 and 5), calcium chloride was calculated towards the pyrometallurgical stage and seemed to indicate that the avoided impacts of lithium reclamation were higher than the added burdens. With calcium chloride included to lithium dust refining, the credit for lithium carbonate was still higher than the impacts in all scenarios and impact indicators, which would suggest that lithium recovery is also environmentally justified.

The chemical inputs to the hydrometallurgical alloy refining process, unlike soda and calcium chloride in lithium recovery, were defined by concentrations, *i.e.*, solution volume, making them more uncertain. The key parameters to consider were the solid/liquid (S/L) ratio in leaching and organic/aqueous (O/A) ratios in the four SX circuits. Although higher S/L would reduce also caustic soda and organic consumption in SX, the ratio was kept at 100 g L^{-1} since the solutions were already highly concentrated. For instance, the leaching solution in *pt-111* contained 47 g L^{-1} cobalt, 49 g L^{-1} nickel, and 3 g L^{-1} copper. The reactions were highly acid consuming. The electrowinning of copper generates acid, so the spent electrolyte was split between the leaching and copper stripping stages to reduce the acid feed. This was sufficient for LFP, but not NMC, and the opportunities to further optimize the leaching stage are therefore limited.

The used O/A ratio was mostly 1 : 1, as reported in the ESI,† but lower ratio in extraction stage would reduce caustic soda and organic consumption, and higher ratio in stripping would affect sulfuric acid and presumably steam consumption in nickel and cobalt recovery. Changes in the other direction would conversely increase the impacts. OD would be the most affected based on the contribution analysis for NMC111 and

Open Access Article. Published on 07 February 2025. Downloaded on 10/26/2025 6:04:00 AM.
This article is licensed under a Creative Commons Attribution 3.0 Unported Licence.

811. Nevertheless, the parameters that affect the inputs and therefore the impact indicators can be recognized from the assessment, which demonstrates how simulations are useful in evaluating uncertainty.

3.4. Sensitivity analysis

Graphite, and aluminum to a lesser degree, were a sufficient energy source for the treatment of NMC black mass (*pt-111* and *pt-811*), but it is also a significant material fraction in terms of recoverable battery weight. Therefore, the effect of recovering graphite during pre-treatment by emerging methods, such as flotation[51–53] were investigated in the simulation so that 90% of the carbon is separated and reclaimed. The downstream treatment of the anode fraction to useful products was excluded from the boundaries, and therefore no credits were provided, either. The results are therefore only reflective of how the change in feedstock affects the pyrometallurgical–hydrometallurgical process.

The calculated compositions of the black masses were calculated with a simple mass balance and are available in Table S7,† and the compositions are very highly concentrated (>95%) cathode material concentrates. The clear benefit from recovering carbon already in the pretreatment phase was that was total cell mass recoveries (%) increased from ~40% to ~70% for NMC, and 20% to 46% LFP battery waste. Therefore the 70% battery mass recovery target according to battery regulation easily achieved by NMC chemistries (approximately 80%) and close even for LFP (66%). The process was no longer autothermal, and the most obvious disadvantage of graphite separation is that an additional reducing agent, such as coke, bio-based carbon,[54] or aluminum scrap,[55] would be required. Coke was assumed to be used as an auxiliary source of reducing power as the most widely used industrial metallurgical reducing agent.

The scenarios presented in Fig. 7 are essentially extensions of the *pt* scenarios where the black mass is low in carbon. The most significant change in the LCI (Table S8†) were that coke was now required also for NMC, the consumption of air and natural gas increased, whereas total electricity decreased. The foreground carbon dioxide emissions of both NMC chemistries also decreased, while the emissions from LFP processing increased.

Fig. 7 demonstrates the change in the impacts (± %) from *pt* scenarios if graphite is reclaimed prior to pyrometallurgical processing, and the effect was substantial particularly in terms of HTc (+250% NMC, +73% LFP). Counterintuitively, the climate change impacts of NMC111 and NMC811 slightly decreased (−6%): the original black mass with graphite contained excess carbon than needed for the reactions and the rest was only converted to heat and carbon dioxide. In the low-carbon black mass, the amount of needed carbon was calculated exactly. The change in CC was, nevertheless, virtually insignificant. The indirect impacts of coke production were more pronounced particularly in toxicity.

The recovery credits were essentially unaffected by the reclamation of graphite since graphite was not credited in this study. The only change was in the process impacts, which mainly increased. The net impacts remained nevertheless remained negative (*i.e.*, implying benefits) for all NMC111 and NMC811 with the exception of OD for 811, which was positive already in the baseline analysis. The baseline *pt-LFP* showed net positive impacts for climate change, which also remained positive in the sensitivity analysis, in addition to which HTc and OD turned positive with the recovery of graphite.

The conclusions remained largely unchanged in terms of the environmental impacts after the separation of graphite given that the process still appears to have lower impacts than the extraction of virgin materials. The analysis would also

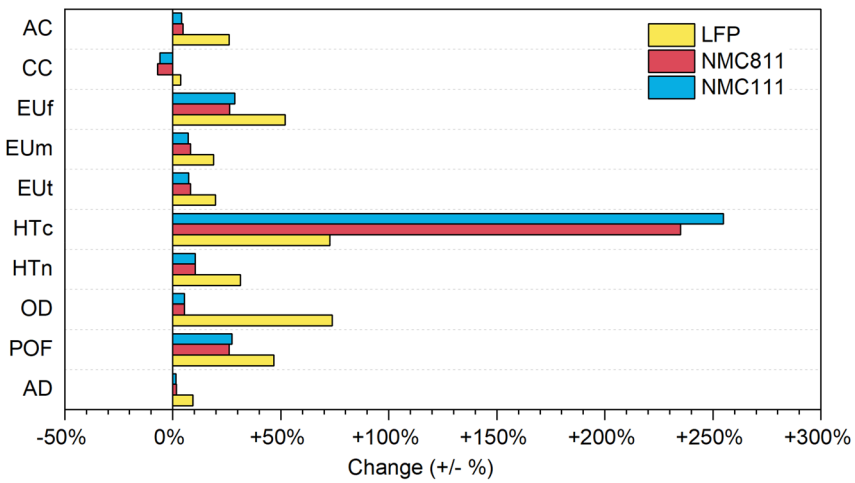

Fig. 7 The effect of separating and recovering graphite from the black mass during pre-treatment, *vs.* graphite-rich black mass in *pt-111*, *pt-811*, and *pt-LFP*. AC refers to acidification, CC to climate change, EUf to eutrophication (freshwater), EUm eutrophication (marine), EUt eutrophication (terrestrial), HTc human toxicity (cancer), HTn human toxicity (non-cancer), OD ozone depletion, POF photochemical ozone formation, and AD abiotic depletion.

Open Access Article. Published on 07 February 2025. Downloaded on 10/26/2025 6:04:00 AM.
This article is licensed under a Creative Commons Attribution 3.0 Unported Licence.

suggest that the results would not change if a minor amount of coke is fed to the processing of graphite-containing NMC materials. It is, however, worth questioning if a complex pyrometallurgical–hydrometallurgical flowsheet is required for the processing of low-graphite black mass containing 98% active cathode material. Direct hydrometallurgical processing without pyrometallurgy or emerging direct recycling flowsheets may be more feasible for low-carbon black masses regardless of any perceived benefits.

4. Conclusions

Process simulation and LCA were combined to evaluate the environmental impacts of emerging pyrometallurgical NMC and LFP battery recycling and to determine further development needs to reach the European battery recycling targets in 2031. The process was studied with and without pre-treatment, and the rest of the flowsheet consists of pyrometallurgical reducing smelting, alloy refining, and the volatilization and refining of lithium. The recovered metals were copper, nickel, cobalt, lithium, and aluminum when the optional pre-treatment is used. The effect of graphite recovery prior to pyrometallurgical processing was studied in a separate scenario analysis. Using process simulation in inventory data gathering enabled a very detailed analysis of how different factors in the feed chemistry or process parameters affected the environmental impacts.

The comparison of recycling and primary material production impacts indicates that the pyrometallurgical recycling of NMC111 and NMC811 is beneficial from an environmental perspective, and the treatment of LFP batteries also reduces the environmental impacts in most of the studied impact categories particularly when the waste batteries pre-treated. Although pyrometallurgical processing is often stated to be energy-intensive, the process was shown to be self-sustaining for NMC cells and black mass due to the presence of graphite in the materials. The pyrometallurgical processing of LFP, while somewhat beneficial in comparison to primary raw materials, did not seem like an attractive option due to the generation of large amounts of slag with very little alloy to refine and recover The avoided impacts from metal recycling were largely dominated by cobalt recovery, but the process impacts were similar regardless of the studied cathode chemistry. This indicates that the recycling of low and entirely non-cobalt chemistries may be more challenging in an environmentally acceptable manner in future.

In terms of the recovery targets: 70% lithium, 95% copper, nickel, and cobalt, 70% battery weight, only copper and lithium were easily reached, while nickel and particularly cobalt may require more effort due to the cumulative losses in pre-treatment, reduction smelting, and hydrometallurgical stages. It is also noteworthy that manganese remains overlooked in research and was not considered at all. The battery weight goal was not reached in any scenario without graphite recovery, but 70% may be manageable for NMC batteries without radical changes in the process particularly with pre-treatment. Improvements in pre-treatment may also be foreseen to improve the overall recoveries given that this study assumed the mechanical treatment losses to be static, which is not the case.

Pre-treatment was demonstrated to reduce the impacts of pyrometallurgical battery recycling, but it also appears to be necessary in order to reach the process recovery targets set by the European Commission especially in the longer term. The benefit of battery pre-treatment was that it reduced the volume of material entering the downstream process but also enabled aluminum recovery, leading to additional credits. To reach the specified 70% battery weight recovery, more advanced processes are still needed, and graphite recovery would be particularly advantageous due to its high share in the batteries. Although opportunities for improvement were recognized, the development of more efficient pyrometallurgical processes is complicated by heterogeneity in cathode chemistries and challenges in the recovery of manganese and graphite.

The disadvantage of implementing the pre-treatment step is that it increases the complexity of the overall process flowsheet, particularly when a specific benefit of traditional pyrometallurgical processing is that this complexity can be avoided. Nevertheless, pyrometallurgical processes alleviate some challenges in hydrometallurgical processing, such as hydrofluoric acid formation potential, and the separation of iron an aluminum from solutions. The separation of graphite during pre-treatment results in a black mass that is very concentrated in cathode material, and in this case complex and capital-intensive pyrometallurgical recycling may no longer be competitive against hydrometallurgical or emerging direct recycling processes, which is worth further investigation.

Author contributions

Marja Rinne: conceptualization, data curation, formal analysis, investigation, visualization, writing: original draft; Heikki Lappalainen: conceptualization, validation, writing – review & editing; Mari Lundström: supervision, project administration, writing – review & editing.

Data availability

The data supporting this article has been included as part of the ESI.†

Conflicts of interest

We have no conflicts of interest to disclose.

Acknowledgements

The study was supported by Horizon Europe-funded RESPECT project (grant agreement id 101069865), Business Finland's BATCircle3.0 project (grant number 1754/31/2024), and the

Open Access Article. Published on 07 February 2025. Downloaded on 10/26/2025 6:04:00 AM.
This article is licensed under a Creative Commons Attribution 3.0 Unported Licence.

Academy of Finland's RawMatTERS Finland Infrastructure (RAMI) based at Aalto University.

References

1 B. Bille, The Hague Centre for Strategic Studies, 2024, https://hcss.nl/report/lithium-supply-security-europe-battery-industry/ (accessed July 5, 2024).
2 A. Zeng, W. Chen, K. D. Rasmussen, X. Zhu, M. Lundhaug, D. B. Müller, J. Tan, J. K. Keiding, L. Liu, T. Dai, A. Wang and G. Liu, *Nat. Commun.*, 2022, **13**, 1341.
3 R. Sommerville, P. Zhu, M. A. Rajaeifar, O. Heidrich, V. Goodship and E. Kendrick, *Resour., Conserv. Recycl.*, 2021, **165**, 105219.
4 D. L. Thompson, J. M. Hartley, S. M. Lambert, M. Shiref, G. D. J. Harper, E. Kendrick, P. Anderson, K. S. Ryder, L. Gaines and A. P. Abbott, *Green Chem.*, 2020, **22**, 7585–7603.
5 S. Kim, J. Bang, J. Yoo, Y. Shin, J. Bae, J. Jeong, K. Kim, P. Dong and K. Kwon, *J. Cleaner Prod.*, 2021, **294**, 126329.
6 D. Latini, M. Vaccari, M. Lagnoni, M. Orefice, F. Mathieux, J. Huisman, L. Tognotti and A. Bertei, *J. Power Sources*, 2022, **546**, 231979.
7 G. Van Hoof, B. Robertz and B. Verrecht, *Metals*, 2023, **13**(12), 1915, DOI: 10.3390/met13121915.
8 D. Cheret and S. Santén, *European Pat*, EP1589121B1, 2008.
9 G. Ren, S. Xiao, M. Xie, B. Pan, J. Chen, F. Wang and X. Xia, *Trans. Nonferrous Met. Soc. China*, 2019, **27**(2), 450–456, DOI: 10.1016/S1003-6326(17)60051-7.
10 L. Scheunis and W. Callebaut, *Singapore Pat*, SG11202105303VA, 2019.
11 C. T. Matos, F. Mathieux, L. Ciacci, M. C. Lundhaug, M. F. Godoy León, D. B. Müller, J. Dewulf, K. Georgitzikis and J. Huisman, *J. Ind. Ecol.*, 2022, **26**, 1261–1276.
12 D. Karabelli, S. Kiemel, S. Singh, J. Koller, S. Ehrenberger, R. Miehe, M. Weeber and K. P. Birke, *Front. Energy Res.*, 2020, **8**, 594857.
13 N. Fallah and C. Fitzpatrick, *J. Energy Storage*, 2023, **68**, 107740.
14 N. Muralidharan, E. C. Self, M. Dixit, Z. Du, R. Essehli, R. Amin, J. Nanda and I. Belharouak, *Adv. Energy Mater.*, 2022, **12**, 2103050.
15 Y. Tian, G. Zeng, A. Rutt, T. Shi, H. Kim, J. Wang, J. Koettgen, Y. Sun, B. Ouyang, T. Chen, Z. Lun, Z. Rong, K. Persson and G. Ceder, *Chem. Rev.*, 2020, **121**, 1623–1669.
16 ISO 14040:2006/A1:2020:en, *Environmental management – Life cycle assessment, principles, and framework. Amendment* 2 (ISO 14040:2006/Amd 1:2020), 2020.
17 ISO 14044:2006/A1:2020:en, *Environmental management – Life cycle assessment, requirements and guidelines. Amendment* 2 (ISO 14040:2006/Amd 1:2020), 2020.
18 Y. Cao, L. Li, Y. Zhang, Z. Liu, L. Wang, F. Wu and J. You, *Resour., Conserv. Recycl.*, 2023, **188**, 106689.
19 E. Kallitsis, A. Korre and G. H. Kelsall, *J. Cleaner Prod.*, 2022, **371**, 133636.
20 M. Mohr, J. F. Peters, M. Baumann and M. Weil, *J. Ind. Ecol.*, 2020, **24**(6), 1310–1322.
21 J. Šimaitis, S. Allen and C. Vagg, *J. Ind. Ecol.*, 2023, **27**(5), 1291–1303.
22 Y. Tao, Z. Wang, B. Wu, Y. Tang and S. Evans, *J. Cleaner Prod.*, 2023, **389**, 136008.
23 H. Yang, X. Hu, G. Zhang, B. Dou, G. Cui, Q. Yang and X. Yan, *Waste Manage.*, 2024, **178**, 168–175.
24 M. A. Rajaeifar, M. Raugei, B. Steubing, A. Hartwell, P. A. Anderson and O. Heidrich, *J. Ind. Ecol.*, 2019, **25**(6), 1560–1571.
25 M. Rinne, R. Aromaa-Stubb, H. Elomaa, A. Porvali and M. Lundström, *Int. J. Life Cycle Assess.*, 2024, **29**, 1582–1597.
26 Metso, *HSC Chemistry software*, 2024, https://www.metso.com/portfolio/hsc-chemistry/(Accessed July 5, 2024).
27 Q. Dai, J. Spangenberger, S. Ahmed, L. Gaines, J. C. Kelly and M. Wang, *EverBatt: A closed-loop battery recycling cost and environmental impacts model*, Argonne National Library, 2019.
28 Green Delta, OpenLCA, 2024, https://www.openlca.org/ (accessed July 8, 2024).
29 Ecoinvent, Ecoinvent 3.10, 2024, https://ecoinvent.org/ecoinvent-v3-10/ (accessed July 8, 2024).
30 J. Marie and S. Gifford, in *Developments in lithium-ion battery cathodes*, Faraday Insights, 2018, p. 18.
31 Global EV outlook 2022, IEA, 2022, https://www.iea.org/reports/global-ev-outlook-2022 (accessed July 5, 2024).
32 W. Schade, I. Haug and D. Berthold, *The future of the automotive sector – Emerging battery value chains in Europe*, ETUI Research paper – report 2022.02, 2022. DOI: 10.2139/ssrn.4220540.
33 J. Kortelainen, *Fortum akkukierrätykseen Saksassa*, Energiauutiset, 2021, https://www.energiauutiset.fi/kategoriat/markkinat/fortum-akkukierratykseen-saksassa.html (accessed July 18, 2024).
34 Northvolt produces first fully recycled battery cell – looks towards establishing 125 000 ton per year giga recycling plant, 2021, https://northvolt.com/articles/recycled-battery/ (accessed July 18, 2024).
35 A. Vanderbruggen, N. Hayagan, K. Bachmann, A. Ferreira, D. Werner, D. Horn, U. Peuker, R. Serna-Guerrero and M. Rudolph, *ACS EST Eng.*, 2022, **2**, 2130–2141.
36 C. Liu, J. Lin, H. Cao, Y. Zhang and Z. Sun, *J. Cleaner Prod.*, 2019, **228**, 801–813.
37 B. Makuza, Q. Tian, X. Guo, K. Chattopadhyay and D. Yu, *J. Power Sources*, 2021, **491**, 229622.
38 H. Dang, N. Li, Z. Chang, B. Wang, Y. Zhan, X. Wu, W. Liu, S. Ali, H. Li, J. Guo, W. Li, H. Zhou and C. Sun, *Sep. Purif. Technol.*, 2020, **233**, 116025.
39 S. Xiao, G. Ren, M. Xie, B. Pan, Y. Fan, F. Wang and X. Xia, *J. Sustain. Metall.*, 2019, **3**, 703–710.
40 Y. Jian, Z. Zongliang, Z. Gang, J. Liangxing, L. Fangyang, J. Ming and L. Yangqing, *Hydrometallurgy*, 2021, **203**, 105638.
41 D. Zhang, X. Zhou, C. Liu and G. Lu, *J. Cryst. Growth*, 2021, **556**, 125989.

 This journal is © The Royal Society of Chemistry 2025

Open Access Article. Published on 07 February 2025. Downloaded on 10/26/2025 6:04:00 AM.
This article is licensed under a Creative Commons Attribution 3.0 Unported Licence.

42 S. K. Sahu, A. Agrawal, B. D. Pandey and V. Kumar, *Min. Eng.*, 2005, **17**(7–8), 949–951.
43 F. Pagnanelli, E. Moscardini, P. Altimari, T. A. Atia and L. Toro, *Waste Manage.*, 2015, **51**, 214–221.
44 Y. Tang, J. Wang and Y. Shen, *Minerals*, 2023, **13**(2), 285, DOI: 10.3390/min13020285.
45 A. De Vita, P. Capros, M. Kannavou, T. Fotiou, P. Siskos, I. Tsiropoulos, N. Katoufa, I. Mitsios, S. Evangepoulou, G. Asimakopoulou, T. Kalokyris, L. Paroussos, K. Fragkiadakis, P. Karkatsoulokis, L. Höglund-Isaksson, W. Winiwarter, P. Purohit, A. Gómez-Sanabria, P. Rafaj, L. Warnecke, A. Deppermann, M. Gusti, S. Frank, P. Lauri, F. di Fulvio, N. Forsell, P. Havlík, P. Witzke and M. Kesting, EU reference scenario 2020 – Energy, transport and GHG emissions – Trends to 2050, European Commission, Publications Office, 2021. https://data.europa.eu/doi/10.2833/35750.
46 Regulation (EU) 2023/1542 of the European Parliament and of the Council of 12 July 2023 concerning batteries and waste batteries, amending Directive 2008/98/EC and Regulation (EU) 2019/1020 and repealing Directive 2006/66/EC, Official Journal, 2023, L191, 1–117.
47 P. M. Kobylin, H. Sippola and P. A. Taskinen, *Calphad*, 2013, **40**, 41–47.
48 M. V. Charykova, V. G. Kriyovichev and W. Depmeier, *Geol. Ore Depos.*, 2010, **52**(8), 701–710, DOI: 10.1007/s11367-019-01723-6.
49 J. B. Dunn, L. Gaines, J. Sulliwan and M. Q. Wang, *Environ. Sci. Technol.*, 2012, **46**, 12704–12710.
50 M. Rinne, H. Elomaa, A. Porvali and M. Lundström, *Resour., Conserv. Recycl.*, 2021, **170**, 105586.
51 M. Abdollahifar, S. Doose, H. Cavers and A. Kwade, *Adv. Mater. Technol.*, 2023, **8**, 3300468.
52 H. Sahivirta, B. P. Wilson, M. Lundström and R. Serna-Guerrero, *Waste Manag.*, 2024, **180**, 96–105.
53 A. Vanderbruggen, N. Hayagan, K. Bachmann, A. Ferreira, D. Werner, D. Horn, U. Peuker, R. Serna-Guerrero and M. Rudolph, *ACS EST Eng.*, 2022, **2**(11), 2130–2141, DOI: 10.1021/acsestengg.2c00177.
54 K. Avarmaa, M. Järvenpää, L. Klemettinen, M. Marjakoski, P. Taskinen, D. Lindberg and A. Jokilaakso, *Metals*, 2020, **6**(4), 58, DOI: 10.3390/batteries6040058.
55 D. C. Nababan, R. Mukhlis, Y. Durandet, L. H. Prentice, W. D. A. Rickard, M. I. Pownceby and M. A. Rhamdhani, *Metall. Mater. Trans. B*, 2024, **55**, 144–167.